Desalination and Water Treatment
www.deswater.com
doi: 10.1080/19443994.2013.797133

51 (2013) 7036–7047
November

Taylor & Francis
Taylor & Francis Group

Response surface methodology for modeling and optimizing the treatment of synthetic starchy wastewater using hydrophilic PES membrane

A. Hedayati Moghaddam[a], J. Shayegan[b,*], J. Sargolzaei[a], T. Bahadori[b]

[a]*Department of Chemical Engineering, Ferdowsi University of Mashhad, Mashhad, Iran*
[b]*Department of Chemical and Petroleum Engineering, Sharif University of Technology, Tehran, Iran*
Tel. +98 2166165420; Fax: +98 2166022751; email: shayegan@sharif.edu

Received 10 August 2011; Accepted 25 February 2013

ABSTRACT

In this work, the process of starch removal from starchy wastewater using a hydrophilic polyethersulfone membrane was investigated. The pore size of the membrane was 0.65 μm and the pattern of stream in plate and frame handmade membrane module was cross-flow. To design the layout of the experiments, response surface methodology was applied. The performance of the filtration process was evaluated by calculating the (chemical oxygen demand) COD removal percentage (rejection factor) and permeate flux. In this study, five operative parameters were investigated, including trans-membrane pressure, flow rate and temperature of feed, pH, and the COD concentration of starch wastewater. Two models were obtained from experimental data, capable of predicting COD removal percentage and permeate flux in different conditions. To check the precision of the models, analysis of variance combined with F-test was carried out. The predicted values obtained from the regression models were close to the actual ones. According to the models, the optimum condition for achieving a high percentage of COD removal and high value of permeate flux was obtained by using mathematical optimization.

Keywords: Starch; Removal; Membrane; COD removal percentage; Permeate flux; Optimization

1. Introduction

The wastewater originated from traditional starch industries are characterized by high chemical oxygen demand (COD) content, ranging from 2,000 to 24,000 mg/L [1–4]. Many attempts have already been reported to treat this kind of wastewater in using biological systems [5–9]. It is worth noting that membrane technology is conveniently applied in water and wastewater treatment [10–12]. Recently, considerable reductions in the price of membranes and the advances in membrane technology have made this approach more practical for separating even smaller starch molecules [13,14]. Applying this technology to starchy wastewater not only significantly reduces its COD content but also improves the cost-effectiveness of the starch industry. Cancino et al. [13] used a hydrophilic membrane to treat corn starch wastewater in a pilot test. Their investigation was divided into two types of membrane technologies. First, they treated the wastewater for 4 h using a microfiltration (MF) module with a pore size of 0.2 μm at a

*Corresponding author.

trans-membrane pressure (TMP) of 250 kPa. The permeate contained only 17% of original wastewater biological oxygen demand (BOD_5), and the permeate flux achieved during MF was around $10.8 \times 10^{-6}\,m^3/m^2h$. Secondly, they used a laboratory reverse osmosis (RO) module to remove higher amounts of BOD_5. Resulted permeate flux had only 0.2% of original wastewater BOD_5 [13]. Sarka et al. [14] by using MF and RO membranes investigated the possibilities of recycling the concentrated retentate back into the production process. They used a ceramic membrane with a filtration area of $0.35\,m^2$ and pore size of 500 and 100 nm as MF, respectively. Permeate flux above $100\,L/m^2h$ was achieved for the 100 nm membrane, but fouling was considerable. They reported that COD and BOD_5 had removal percentages of about 60% [14]. It is worth noting that ceramic membranes are relatively expensive. In these studies, the optimum condition was not obtained since the process was investigated in a single condition and the effects of parameters on process performance were not studied. The most important parameter in membrane-based treatment is pore size; starchy wastewater should be treated using membranes with a pore size smaller than the diameter of the starch molecule. The starch granules size may vary from 1 to 50 μm [15]. Accordingly, selecting a commercial membrane with the pore size of 0.65 μm seems acceptable for complete filtration. The range of gelatinization temperature of starch spans from 60 to 80°C [16,17]. Despite the fact that membrane technology has many advantages, including being energy-saving and environmentally friendly, there are several drawbacks in using this technology. The main drawback is permeate reduction over time, which is mainly due to membrane fouling and concentration polarization [18,19]. Membrane fouling also changes the membrane selectivity and decreases the overall process productivity [20]. To overcome this problem, optimal process conditions that simultaneously maximize both the rejection factor and permeate flux must be identified.

In many experiments, the outputs depend not only on operating parameters but also on the interactions between the input parameters which may affect the output responses. So, these possible interactions must be taken into consideration. The performance of membrane separation is a complex and sensitive function of numerous parameters, and using a systematic approach is necessary to model the process and obtain optimum conditions. The interactions could not be considered by varying one parameter and keeping the others constant. This problem has been resolved by a design of experiment (DoE) technique. The use of DoE has been expanded in recent years in several fields of science and engineering [21–30]. This technique is divided into several subsets. One of the useful methods used in this study is response surface methodology (RSM). RSM is a mathematical method for modeling the experimental data. The present study describes experimental and statistical approaches to model and optimize the separation of starch from synthetic starchy wastewater. The process was analyzed and modeled using RSM. The parameters examined were TMP, flow rate, temperature, pH, and starch concentration. The effects of these parameters on membrane performance were assessed. The innovation of this work was developing a methodology for performing an efficient separation. A novel and comprehensive approach was developed by employing two proposed responses as the measure of separation efficiency and fouling reduction termed COD removal percentage and permeate flux, respectively.

2. Materials and methods

2.1. Materials

The main materials in this experiment were sodium hydroxide (NaOH) and chloridric acid (HCl) that were used in backwash procedures, as well as starch (food grade) for preparing synthetic wastewater. A plate and frame module was made of steel to hold a sheet of commercialized hydrophilic polyethersulfone[1] (PES) membrane. PES membrane is, in essence, a hydrophobic membrane with low resistant fouling, which leads to severe permeate flux decline during running the experiments [31]. But by treating this type of membrane, its hydrophobic property would change to the hydrophilic one that was suitable for this research [32]. A centrifugal pump (Victory KM100) with a maximum head of 50 m and maximum flow rate of 50 L/min and a flow meter with a maximum capacity of 20 L/min were also used.

2.2. Response surface methodology (RSM)

RSM is a combination of mathematical and statistical techniques that are useful for analyzing and modeling a set of data, in which some responses of interest are influenced by several variables. The main goal of this method is optimization of these responses [33]. RSM provides an environment to study the parameters and their interaction effects on output responses and finally, extracts a mathematical model that is useful in plotting the effect of parameters and

[1]©1995–2011 General Electric Company, http://www.geosmolabstore.com.

their interactions. There are several statistical design techniques associated to RSM such as three levels of factorial design, central composite design (CCD), and hexagonal design. The three groups of design points are involved in a CCD are:

- two-level factorial or fractional factorial design (FFD) points
- axial points
- center points

Using CCD, the number of experiments is achieved by the following equation:

$$N = N_f + N_a + N_c \quad (1)$$

where N is the total number of experiments, N_f is the number of factorial design, N_a is the number of axial points, and N_c is the number of center points. There is no exact rule to determine the number of center points. In this study, N_c was adjusted to six. It is noteworthy that N_f and N_a were achieved from Eqs. (2) and (3), respectively.

$$N_f = 2^n \quad (2)$$

$$N_a = 2 \times n \quad (3)$$

where n is the number of parameters involved.

Eq. (1) shows that by increasing the input parameters, the number of experiments will increase rapidly. By using the FFD to screen the insignificant parameters, the number of input parameters decreases and the number of experiments planned via CCD would decrease consequently. A two-level FFD was employed to screen the insignificant parameters. If the response behavior is moderately nonlinear, a quadratic model may be appropriate. CCDs are designed to estimate the coefficients of a quadratic model. All point descriptions will be in terms of coded values of the parameters. In other words, data processing is accomplished in coded terms. There are several types of software in this field. The investigator can also analyze the response surface data with paper and pencil, but this is time-consuming. In this study, we used Design Expert[2] software to develop the experimental plan for analyzing the collected data and to perform the analysis of variance (ANOVA).

A parameter named alpha will be introduced in CCD that represents axial distance. The value of axial distance determines the location of star points in a CCD. Alpha, the distance from centre point to star point, has the maximum value of $2^{n/4}$, where n is the number of factors [34,35]. In this work, four parameters have been investigated. Accordingly, the maximum value of alpha would be two. But, to avoid allocating a negative value for low level point (star point), the default value of Design Expert software for axial distance (1.41) has been selected.

Alpha is usually somewhat larger than one. In this study, alpha was 1.41. The related graphs were plotted using MATLAB software. In an ANOVA table, a good model must be significant and the lack-of-fit must be insignificant.

2.3. Experimental analysis

RSM has four major steps: experimental design, model fitting, model validation, and condition optimization. As mentioned earlier, experimental designs such as CCD are useful for RSM because they do not require an excessive number of experimental runs [36]. Operating parameters were coded according to the following equation [37]:

$$C_i = \frac{x_i - \frac{x_{i,high} + x_{i,low}}{2}}{\frac{x_{i,high} - x_{i,low}}{2}} \quad (4)$$

where C_i is the coded value of the natural independent variable x_i, $x_{i,high}$ and $x_{i,low}$ are the values of variables at high and low levels, respectively.

In order to screen the insignificant parameters, a 2^{5-2} FFD with three replicates at the center point was performed [38].

According to ANOVA table for COD removal percentage and permeate flux, which were obtained by FFD, it is obvious that TMP has no effect on COD removal percentage but has a positive effect on permeate flux. So, this parameter could be set at a maximum value to increase the permeate flux and consequently decrease the number of parameters that result in removing 18 experiments. As mentioned earlier, CCD is comprised of three groups of design points. The factorial portion is a full factorial design with all combinations of parameters at two levels, the center points, which is the midpoint between the high and low levels, were repeated six times, and the axial or star points were adjusted according to an alpha value of 1.41. So, the number of experiments obtained from Eq. (1) was 30. Processing parameters involved in CCD are depicted in Table 1. The design layout and experimental results of RSM for COD removal

[2]©Vaughn, N.A., et al., Design-Expert(R), Version 8 for Windows, Stat-Ease, Inc., Minneapolis, 2011, web site: http://www.statease.com.

Table 1
Processing parameters involved in CCD

Process variables	Code	$-\alpha$	-1	0	1	α	Variation interval
Flow (L/min m^2)	A	2.96	4	6.5	9	10.04	2.5
Temperature (°C)	B	20.20	26	40	54	59.80	14
pH	C	6.78	7.5	9.25	11	11.72	1.75
Concentration (g/L)	D	0.17	1	3	5	5.83	2

Table 2
The design layout and experimental results of RSM

Standard run no.	Run	Block	Flow-A	Temp.-B	pH-C	Conc.-D	Permeate flux (L/min m^2)	COD removal (%)
1	26	1	4.00	26.00	7.50	1.00	1.75	86.5
2	5	1	9.00	26.00	7.50	1.00	1.63	84.8
3	29	1	4.00	54.00	7.50	1.00	1.77	95.2
4	22	1	9.00	54.00	7.50	1.00	0.87	92.3
5	15	1	4.00	26.00	11.00	1.00	0.97	84.3
6	12	1	9.00	26.00	11.00	1.00	1.52	81.3
7	23	1	4.00	54.00	11.00	1.00	1.71	91.5
8	3	1	9.00	54.00	11.00	1.00	1.12	89.2
9	2	1	4.00	26.00	7.50	5.00	1.05	92.4
10	11	1	9.00	26.00	7.50	5.00	0.89	89
11	4	1	4.00	54.00	7.50	5.00	1.06	97.5
12	6	1	9.00	54.00	7.50	5.00	0.36	97
13	1	1	4.00	26.00	11.00	5.00	0.62	89.3
14	8	1	9.00	26.00	11.00	5.00	1.35	86.6
15	28	1	4.00	54.00	11.00	5.00	0.97	90.2
16	9	1	9.00	54.00	11.00	5.00	2.3	91
17	21	1	2.96	40.00	9.25	3.00	0.52	92
18	19	1	10.04	40.00	9.25	3.00	2.42	88
19	7	1	6.50	20.20	9.25	3.00	0.88	84.3
20	17	1	6.50	59.80	9.25	3.00	2.2	96.4
21	16	1	6.50	40.00	6.78	3.00	1.22	91.5
22	27	1	6.50	40.00	11.72	3.00	1.73	88.4
23	24	1	6.50	40.00	9.25	0.17	1.3	88
24	20	1	6.50	40.00	9.25	5.83	1.83	93.5
25	10	1	6.50	40.00	9.25	3.00	1.75	90.1
26	30	1	6.50	40.00	9.25	3.00	1.9	92.3
27	25	1	6.50	40.00	9.25	3.00	1.83	89
28	18	1	6.50	40.00	9.25	3.00	1.75	88.7
29	13	1	6.50	40.00	9.25	3.00	1.63	91
30	14	1	6.50	40.00	9.25	3.00	1.77	92.5

percentage and permeate flux are summarized in Table 2.

Root mean square error (RMSE) represents the square root of the average squared difference between the predicted values estimated from a model and the actual values [39]. RMSE was determined by the following equation:

$$\mathrm{RMSE} = \sqrt{\frac{\sum(Y_{\mathrm{pred.}} - Y_{\mathrm{exp.}})^2}{M}} \quad (5)$$

where Y_{exp} and Y_{pred} were experimental and predicted values, respectively, and M was the total number of data.

3. Results and discussion

3.1. ANOVA analysis and effect of factors on filtration performance

To ensure the accuracy of the current models, some tests are performed to study the significance of the regression model, individual model coefficients, and lack-of-fit. The ANOVA table for assessing the permeate flux is shown in Tables 3 and 4.

Values of *(Prob > F)* less than 0.05 indicate the model terms are significant and values greater than 0.10 indicate they are not significant. The values in the range of 0.05 to 0.10 are transitional. So, according to the ANOVA table for permeate flux, *B*, *C*, *D*, and A^2 are significant model terms. The main effect of flow rate (*A*) is not a significant term, but to present a hierarchic model; this is included in the model. As Ghesh-laghi et al. [37] mentioned, model hierarchy maintains the relationships between main and interaction effects, so models derived in terms of real values from non-hierarchically coded models are incorrect [37]. As is shown in Table 3, there are insignificant terms in ANOVA table. To obtain more accurate model, such terms should be removed since they have no effects on permeate flux. It is important to note that removing these insignificant terms leads to an improved model. So, a backward elimination procedure was selected to automatically reduce the insignificant terms. ANOVA table related to improved model is shown in Table 4. The p-value of model is still been less than 0.05 indicates that the improved model is still significant or the removed terms have no effects on the significance of model, actually. According to an ANOVA table for response surface reduced quadratic model, as depicted in Table 4, the ranking is as follow: $C>B>D>A^2>B^2>A$. Adequate Precision of 19.79 indicates an adequate signal. The Model F-value of 26.68 implies that the model is significant. There is only a 0.01% chance that a Model F-Value this large could occur as a result of noise. The "lack of fit F-value" of 0.97 implies that the lack of fit is not significant relative to pure error. Pure error is a measure of error related to repeatability. In other words, this is the sum of squares of the repeat observations divided by the degree of freedom. There is a 57.14% chance that a "Lack of Fit F-value" this large could occur due to noise. Non-significant lack of fit is good. The integrity of a model can be checked by the determination of R^2 coefficient and adjusted R^2 [40]. In this study, for permeate flux, R^2 is 0.88, implying that 88.82% of response variability is achived by a regression model. R^2 increases as the number of terms increases in the model, while no improvement in model is observed [41]. So to tackle this problem adjusted R^2 was introduced, which would increase only due to the model improvement. In this case adjusted R^2 is 0.85

Table 3
ANOVA table for permeate flux model

Source	Sum of square	Df	Mean square	*F* value	*p*-value	
Model	7.91	14	0.57	8.54	<0.0001	Significant
A-A	3.99E−003	1	3.99E−003	0.06	0.8093	
B-B	2.46	1	2.46	37.22	<0.0001	
C-C	2.53	1	2.53	38.29	<0.0001	
D-D	1.80	1	1.80	27.26	0.0001	
AB	1.00E−004	1	1.00E−004	1.51E−003	0.97	
AC	0.017	1	0.017	0.26	0.62	
AD	4.90E−003	1	4.90E−003	0.07	0.79	
BC	0.02	1	0.02	0.30	0.59	
BD	0.01	1	0.01	0.18	0.67	
CD	0.00	1	0.00	0.00	1.00	
A^2	0.61	1	0.61	9.28	0.01	
B^2	0.16	1	0.16	2.44	0.14	
C^2	1.22E−003	1	1.22E−003	0.02	0.89	
D^2	3.22E−003	1	3.22E−003	0.05	0.83	
Residual	0.99	15	0.07		<0.0001	
Lack of fit	0.76	10	0.08	1.62	0.31	Not significant
Pure error	0.23	5	0.05			
Cor total	8.90	29				
Model	7.91	14				

Table 4
ANOVA table for reduced permeate flux model

Source	Sum of square	Df	Mean square	*F* value	*p*-value	
Model	7.85	6	1.31	28.68	<0.0001	Significant
A-A	3.99E−003	1	3.99E−003	0.09	0.77	
B-B	2.46	1	2.46	53.94	<0.0001	
C-C	2.53	1	2.53	55.50	<0.0001	
D-D	1.80	1	1.80	39.51	<0.0001	
A^2	0.65	1	0.65	14.25	0.001	
B^2	0.17	1	0.17	3.70	0.07	
Residual	1.05	23	0.05			
Lack of fit	0.82	18	0.04	0.97	0.57	Not significant
Pure error	0.23	5	0.05			
Cor total	8.90	29				

reasonably in accords with R^2 implies that this value of R^2 is not unreal.The predicted R^2 of 0.76 is in reasonable agreement with an adjusted R^2. The final equation for permeate flux in terms of coded factors obtained from regression of values is as below:

$$\text{Permeate flux} = 1.71 + 0.014 \times A - 0.35 \times B - 0.36 \times C - 0.30 \times D - 0.25 \times A^2 - 0.13 \times B^2 \quad (6)$$

Expression of response in actual values is preferred. So, by converting coded values to actual values using Eq. (4), the following equation in terms of actual value achieved:

$$\text{Permeate flux} = 2.22 + 0.54 \times \text{Flow rate} + 0.028 \times \text{Temperature} - 0.20 \times \text{pH} - 0.15 \times \text{concentration} - 0.04 \times \text{Flow rate}^2 - 6.632 \times 10^{-4} \times \text{Temperature}^2 \quad (7)$$

Subjected to: 3 <Flow rate <10 L/min, 20 <Temperature <60°C, 7.5<pH <11.7 and 0.17<Concentration <5.83 g/L. This model can be used to predict the permeate flux within the limiting bounds of experimental parameters. To check the adequacy of final model, the normal probability plot vs. the studentized residuals is checked and illustrated in Fig. 1. The normal probability plot indicates whether the residuals follow a normal distribution or not. In this case, the points that follow a straight line confirm that errors were normally distributed with a mean of zero. Definite patterns like an "S-shaped" curve indicate that a transformation of response may provide a better analysis.

The residual vs. run number and predicted values were checked to test the assumption of constant variance (not shown). In Figs. 2–4 three-dimensional plots and related contours have been made using Matlab software to reveal the effect of concentration; pH, flow rate and temperature on permeate flux. It is clear that these graphs are drawn according to Eq. (6). In Fig. 2, the permeate flux plot versus flow rate and temperature is illustrated. As it can be observed from this figure, it is clear that terms A^2 and B^2 twist the graph but the effect of A^2 is more severe. The results show that the permeate flux increases as flow rate increases, up to about 6.75 L/min m^2 of flow rate. The reason for this issue may be related to an increase of turbulency. Turbulence at membrane surface - emerges after increasing the flow rate velocity - likely diminishes the concentration polarization. Guerra et al. [42] mentioned same reason for the increase of permeate flux with increasing cross flow velocity during

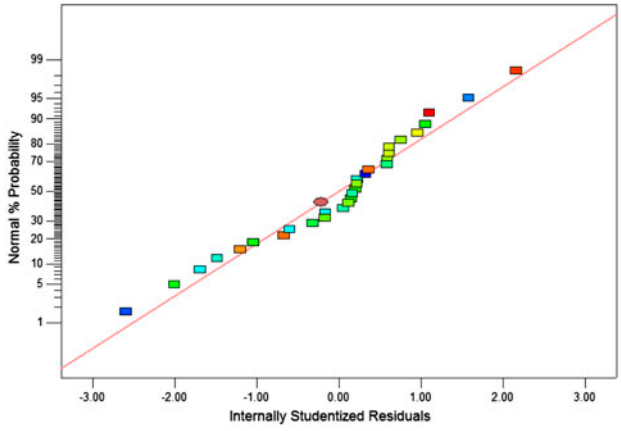

Fig. 1. Normal probability plot of studentized residuals for the permeate flux.

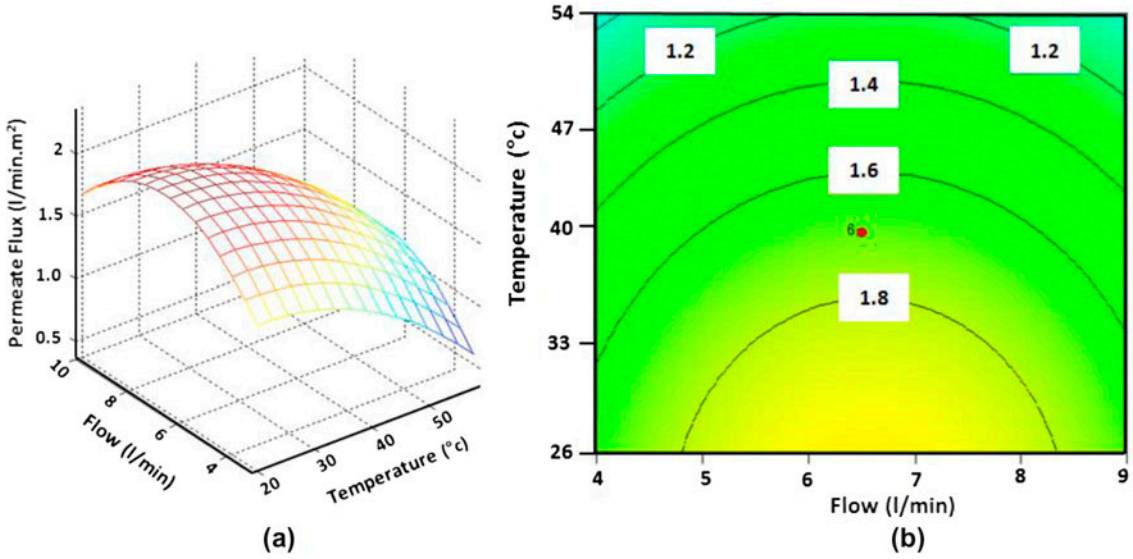

Fig. 2. 3-D (a) and contour plot (b) of predicted permeate flux as a function of flow and temperature at pH = 9 and concentration = 3 g/L.

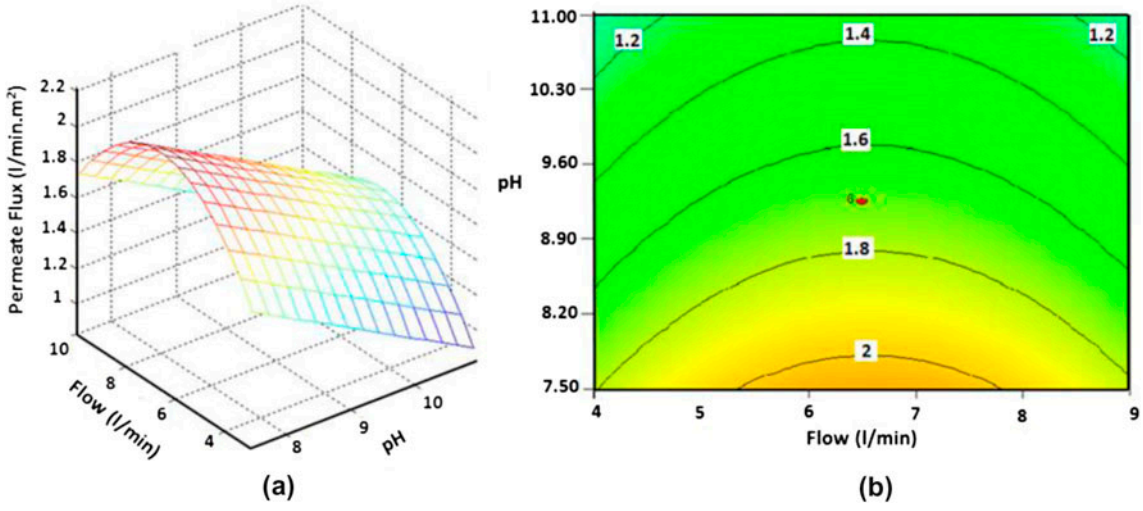

Fig. 3. 3-D (a) and contour plot (b) of predicted permeate flux as a function of flow and pH at temperature = 40°C and concentration = 3 g/L.

investigating the effect of Re number on permeate flux for a ceramic membrane ultrafiltration of surface water [42]. It is obvious that beyond 6.75 L/min m^2 of flow rate, the increase in amount of flow has a reverse effect and there is a marked decrease in permeate flux. This may be due to the fact, that since the value of flow rate is less than 6.75 L/min m^2 increasing the flow rate (cross flow velocity) which enhances particulate removal from membrane surface leads to the increase in permeate flux. But for the values more than 6.75 L/min m^2, the permeate flux is influenced more by irreversible fouling than by concentration polarization. So, increasing the flow rate has no considerable effect on treating fouling and recovering permeate flux. On the other hand, temperature of membrane would increase due to applying high flow rate velocity, which may change the hydrophilic and resistance fouling property of membrane that leads to permeate flux decline. Similar observations can be outlined from Fig. 3.

It is to be noted that concentration and pH have negative effects on permeate flux (Figs. 3 and 4). By increasing the concentration of feed, the concentration polarization phenomenon takes place and leads

to a linear decrease of permeate flux. Increasing the pH of solution results in strengthening the cohesion forces between starch molecules, so that the size of starch molecules grows and the concentration polarization phenomena on the surface of membrane results in lower permeate flux. The response values determined by empirical models were compared to experimental data for permeate flux are shown in Fig. 5. As can be seen, the results obtained from RS model are in good accord with experimental data. Therefore, models can be considered adequate for predictions and optimization.

The value of RMSE for permeate flux was 0.19.

The same method was used to analyze the permeate flux applied for analysis of COD removal. The ANOVA table for COD removal is illustrated in Table 5. In analysis of the values related to COD removal, the R^2 is 0.91 reasonably close to one, which is acceptable and the adjusted R^2 is 0.89. The predicted R^2 is 0.85, which is in reasonable agreement with the adjusted R^2. The adjusted R^2-value is particularly useful when comparing the models with different number of terms. This comparison is, however, done in the background when the model reduction is

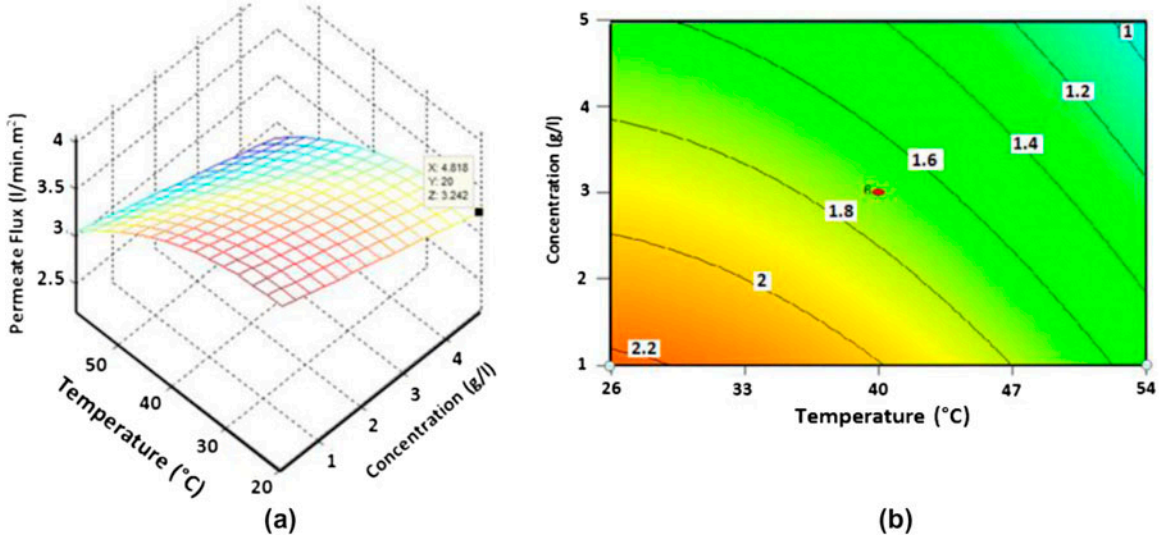

Fig. 4. 3-D (a) and contour plot (b) of predicted permeate flux as a function of temperature and concentration at pH = 9 and flow = 6.5 L/min.

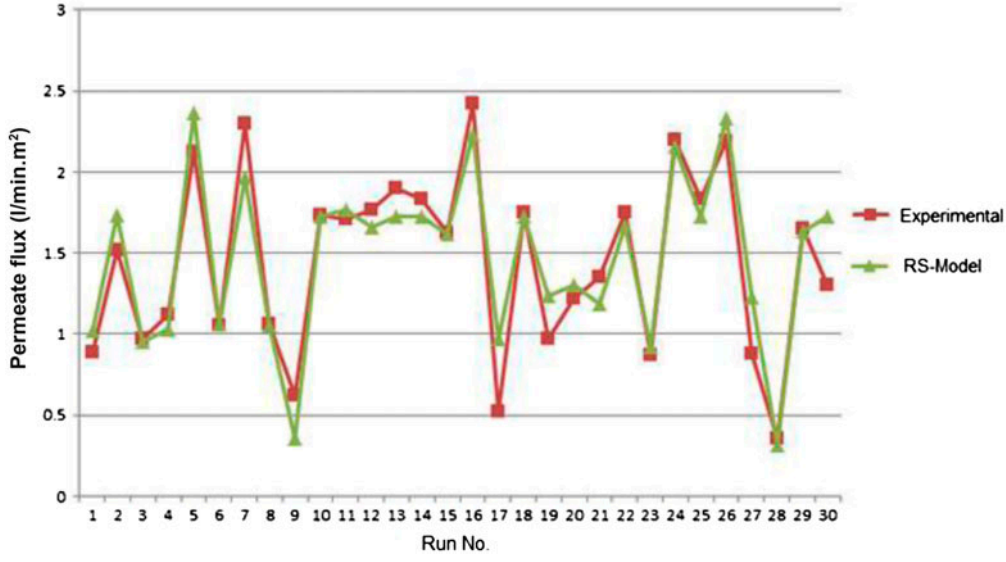

Fig. 5. Experimental data compared to predicted values given by the response surface model for permeate flux.

Table 5
ANOVA table for reduced COD removal model

Source	Sum of square	Df	Mean square	*F* value	*p*-value	
Model	388.66	6	64.78	40.94	<0.0001	Significant
A-A	22.81	1	22.81	14.41	0.0009	
B-B	223.19	1	223.19	141.05	<0.0001	
C-C	63.67	1	63.67	40.23	<0.0001	
D-D	63.65	1	63.65	40.22	<0.0001	
BC	4.95	1	4.95	3.13	0.09	
BD	10.40	1	10.40	6.57	0.017	
Residual	36.40	23	1.58			
Lack of fit	23.32	18	1.30	0.50	0.88	Not significant
Pure error	13.08	5	2.62			
Cor total	425.06	29				

taking place [43]. According to the F-value represented in Table 5, the parameters are ranked in order to their importance as follows: *B*>*C*>*D*>*A*>*BD*>*BC*. The final experimental model in terms of coded factors for COD removal percentage is presented as follows:

$$\text{COD removal}\% = 90.13 - 1.07 \times A + 3.34 \times B - 1.78 \times C + 1.78 \times D - 0.56 \times B \times C - 0.81 \times B \times D \quad (8)$$

In terms of actual factors, the final empirical model for COD Removal is as follows:

$$\text{COD removal}\% = 78.26 - 0.43 \times \text{Flow} + 0.54 \times \text{Temperature} - 0.11 \times \text{pH} + 2.04 \times \text{concentration} - 0.023 \times \text{Temperature} \times \text{pH} - 0.029 \times \text{Temperature} \times \text{Concentration} \quad (9)$$

The response values determined by RS models were compared to experimental data and the results are shown in Fig. 6 for COD removal percentage.

The value of RMSE for COD removal percentage was 1.10.

The COD removal percentage as a function of temperature and pH, is illustrated in Fig. 7. Other factors (flow rate and concentration) were held at a central level 6.5 L/min and 3 g/L, respectively. Despite the existence of an interaction term between temperature and pH, there is no curvature in this case, because the curvature takes place at the points that are out of range. As it can be observed from the figure, the rise

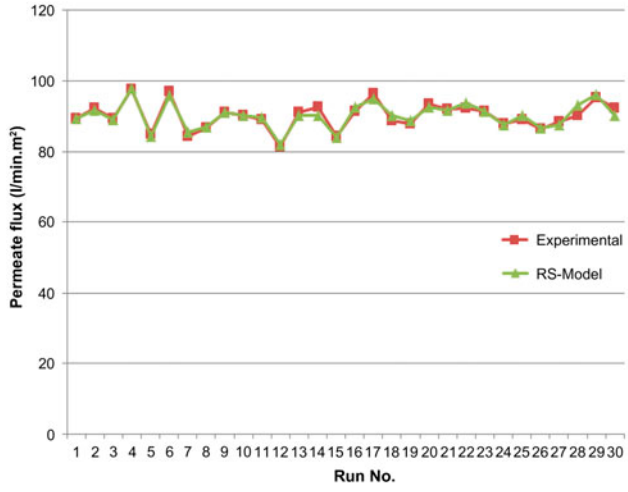

Fig. 6. Experimental data compared to predicted values given by the response surface model for COD removal %.

of pH led to decrease in COD removal percentage, which is explained by the diminishing cohesion forces between starch and membrane. It also results in the decreased tendency to absorb the starch molecules on membrane surface absorbing sites. An increase in temperature had positive significant influence on COD removal percentage, because by raising the temperature, the tendency of starch to move into a gelatinization phase would increase. Consequently, the size growth of starch particles leads to a high percentage of COD removal. Similarly, a contour and 3-D graph of COD removal percentage as a function of temperature and concentration are illustrated in Fig. 8. As shown, the increase in concentration results in an increase in COD Removal percentage. This may be because of the formation of a thicker gel layer on a

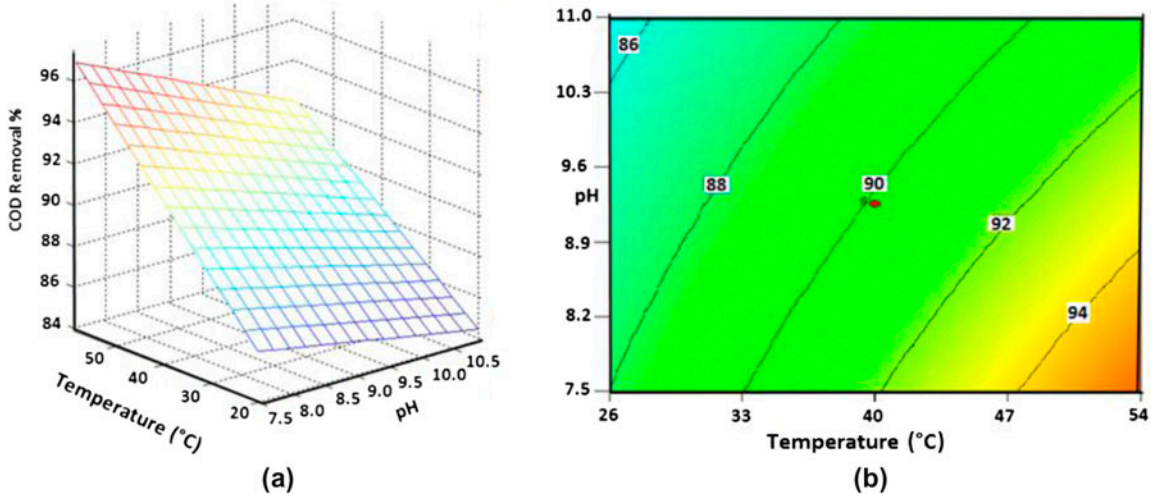

Fig. 7. 3-D (a) and contour plot (b) of predicted COD removal percentage as a function of temperature and pH at concentration = 3 g/L and flow = 6.5 L/min.

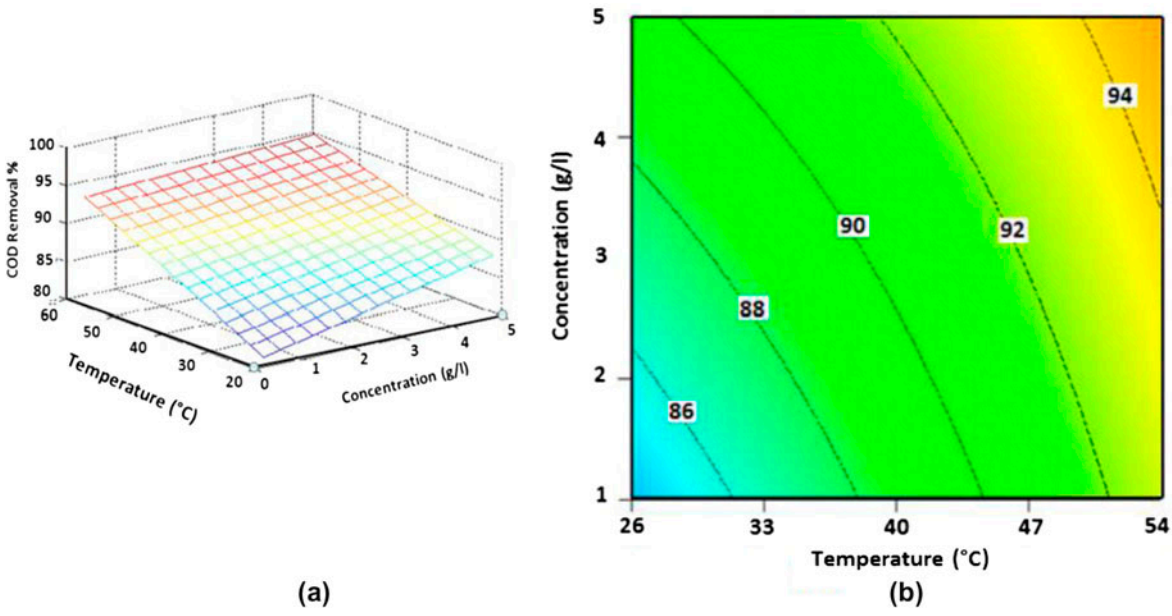

Fig. 8. 3-D (a) and contour plot (b) of predicted COD removal percentage as a function of temperature and concentration at pH = 9 and flow = 6.5 L/min.

membrane surface that advances the performance of the filtration process.

3.2. Optimization

One of the goals of this study was to provide a RSM for optimizing the treatment of starchy industry wastewater by using a membrane process. The useful approach to optimize the multiple responses is to use the simultaneous optimization techniques by applying the created mathematical models. The desirability function approach is one of the most widely used methods in optimizing the multiple response processes. In this method, first, each response y_i converts to an individual desirability function d_i, which varies over the following range:

$$0 \leq d_i \leq 1$$

where if the response y_i is at its goal or target, then $d_i = 1$, and if the response is outside an acceptable

Table 6
Optimized condition and obtained outputs

Flow (L/min)	Temperature (°C)	pH	Concentration (g/L)	COD removal (%)	Permeate flux (L/min m^2)	Desirability
5.92	51.84	7.50	1.00	94.35	1.95	0.79

region, $d_i = 0$. Then the design variables are chosen to maximize the overall desirability as follow:

$$K = (d_1 \times d_2 \ldots d_m)^{1/m}$$

where m is the number of responses [33].

The Design Expert software finds optimum condition, using the desirability function approach. The optimum condition for this process is presented in Table 6.

4. Conclusion

In this research, an investigation was made to describe experimental and statistical approaches to model, and optimize the separation of starch from synthetic starchy wastewater using a plate and frame membrane module. The effects of operative parameters such as flow rate (*A*), temperature (*B*), pH (*C*) and concentration (*D*) on membrane performance were investigated within the design space introduced in the RSM. By comparing the obtained results using RSM to experimental data, it was observed that there is a good agreement between RSM model outputs and experimental data. Finally, by using these models, mathematical optimization was carried out and the optimum condition was obtained. As a result, it is unnecessary to carry out the extensive pilot plant testing for data collection, which can be interpolated with potentially great savings, in terms of both time and cost.

References

[1] O. Chavalparit, M. Ongwandee, Clean technology for the tapioca starch industry in Thailand, J. Clean. Prod. 17 (2009) 105–110.
[2] P. Hien, L. Oanh, N. Viet, G. Lettinga, Closed wastewater system in the tapioca industry in Vietnam, Water Sci. Technol. 39 (1999) 89–96.
[3] F.M. Ferraz, A.T. Bruni, V.L. Del Bianchi, Performance of an Anaerobic Baffled Reactor (ABR) in treatment of cassava wastewater, Braz. J. Microbiol. 40 (2009) 48–53.
[4] P. Rangasamy, I. Pvr, S. Ganesan, Anaerobic tapered fluidized bed reactor for starch wastewater treatment and modeling using multilayer perceptron neural network, J. Environ. Sci. 19 (2007) 1416–1423.
[5] X. Colin, J.L. Farinet, O. Rojas, D. Alazard, Anaerobic treatment of cassava starch extraction wastewater using a horizontal flow filter with bamboo as support, Bioresour. Technol. 98 (2007) 1602–1607.
[6] B. Rajbhandari, A. Annachhatre, Anaerobic ponds treatment of starch wastewater: Case study in Thailand, Bioresour. Technol. 95 (2004) 135–143.
[7] H. Movahedyan, A. Assadi, A. Parvaresh, Performance evaluation of an anaerobic baffled reactor treating wheat flour starch industry wastewater, Iran J. Environ. Health Sci. Eng. 4 (2007) 77–84.
[8] A.P. Annachhatre, P.L. Amatya, UASB treatment of tapioca starch wastewater, J. Environ. Eng. 126 (2000) 1149–1152.
[9] M. Rajasimman, C. Karthikeyan, Aerobic digestion of starch wastewater in a fluidized bed bioreactor with low density biomass support, J. Hazard. Mater. 143 (2007) 82–86.
[10] A. Salahi, R. Badrnezhad, M. Abbasi, T. Mohammadi, F. Rekabdar, Oily wastewater treatment using a hybrid UF/RO system, Desalin. Water Treat. 28 (2011) 75–82.
[11] M. Koenig, N. Selzer, B. Von Harten, Large ultrafiltration system for industrial waste water re-use in Turkey, Desalin. Water Treat. 31 (2011) 82–87.
[12] E. Gasia-Brucha, P. Sehnb, V. García-Molinaa, M. Buscha, O. Raizec, M. Negrinc, Field experience with a 20,000 m^3/d integrated membrane seawater desalination plant in Cyprus, Desalin. Water Treat. 31 (2011) 178–189.
[13] B. Cancino, F. Rossier, C. Orellana, Corn starch waste water treatment with membrane technologies: Pilot test, Desalination 200 (2006) 750–751.
[14] E. Sárka, V. Pour, A. Veselá, Z. Bubník, Possibilities for the use of membrane processes for the pre-treatment of wastewater from the production of dried potato purée, Desalination 249 (2009) 135–138.
[15] B. Svihus, A. Uhlen, O. Harstad, Effect of starch granule structure, associated components and processing on nutritive value of cereal starch: A review, Anim. Feed Sci. Technol. 122 (2005) 303–320.
[16] P. Kampeerapappun, D. Aht-Ong, D. Pentrakoon, K. Srikulkit, Preparation of cassava starch/montmorillonite composite film, Carbohydr. Polym. 67 (2007) 155–163.
[17] L.A. Bello-Perez, E. Agama-Acevedo, S.G. Sayago-Ayerdi, E. Moreno-Damian, J. Figueroa, Some structural, physicochemical and functional studies of banana starches isolated from two varieties growing in Guerrero, Mexico, Starch-Stuttgart 52 (2000) 68–72.
[18] M. Abbasi, R.S. Mohammad, A. Salahi, S. Abbasi, T. Mohammadi, Flux decline and membrane fouling in cross-flow microfiltration of oil-in-water emulsions, Desalin. Water Treat. 28 (2011) 1–7.
[19] C.Y. Tang, P. Yijin, Fouling of ultrafiltration membrane during secondary effluent filtration, Desalin. Water Treat. 30 (2011) 289–294.
[20] M.C. Martí-Calatayud, M.C. Vincent-Vela, S. Álvarez-Blanco, J. Lora-García, E. Bergantiños-Rodríguez, Analysis and optimization of the influence of operating conditions in the ultrafiltration of macromolecules using a response surface methodological approach, Chem. Eng. J. 156 (2010) 337–346.

[21] C. Cojocaru, G. Zakrzewska-Trznadel, A. Jaworska, Removal of cobalt ions from aqueous solutions by polymer assisted ultrafiltration using experimental design approach. part 1: Optimization of complexation conditions, J. Hazard. Mater. 169 (2009) 599–609.
[22] K.M. Desai, S.A. Survase, P.S. Saudagar, S. Lele, R.S. Singhal, Comparison of artificial neural network (ANN) and response surface methodology (RSM) in fermentation media optimization: Case study of fermentative production of scleroglucan, Biochem. Eng. J. 41 (2008) 266–273.
[23] K.P. Singh, S. Gupta, A.K. Singh, S. Sinha, Optimizing adsorption of crystal violet dye from water by magnetic nanocomposite using response surface modeling approach, J. Hazard. Mater. 186 (2011) 1462–1473.
[24] K. Yetilmezsoy, S. Demirel, R.J. Vanderbei, Response surface modeling of Pb (II) removal from aqueous solution by Pistacia vera L.: Box–Behnken experimental design, J. Hazard. Mater. 171 (2009) 551–562.
[25] M. Amini, H. Younesi, N. Bahramifar, A.A.Z. Lorestani, F. Ghorbani, A. Daneshi, M. Sharifzadeh, Application of response surface methodology for optimization of lead biosorption in an aqueous solution by *Aspergillus niger*, J. Hazard. Mater. 154 (2008) 694–702.
[26] P. Sharma, L. Singh, N. Dilbaghi, Response surface methodological approach for the decolorization of simulated dye effluent using Aspergillus fumigatus fresenius, J. Hazard. Mater. 161 (2009) 1081–1086.
[27] G. Sudarjanto, B. Keller-Lehmann, J. Keller, Optimization of integrated chemical–biological degradation of a reactive azo dye using response surface methodology, J. Hazard. Mater. 138 (2006) 160–168.
[28] M. Sultania, J. Rai, D. Srivastava, Process modeling, optimization and analysis of esterification reaction of cashew nut shell liquid (CNSL)-derived epoxy resin using response surface methodology, J. Hazard. Mater. 185 (2011) 1198–1204.
[29] J. Fu, Y. Zhao, Q. Wu, Optimising photoelectrocatalytic oxidation of fulvic acid using response surface methodology, J. Hazard. Mater. 144 (2007) 499–505.
[30] A. Ahmad, C. Leo, S. Shukor, Statistical design of experiments for dye-salt-water separation study using bimodal porous silica/γ-alumina membrane, Desalin. Water Treat. 5 (2009) 80–90.
[31] S. Nakatsuka, I. Nakate, T. Miyano, Drinking water treatment by using ultrafiltration hollow fiber membranes, Desalination 106 (1996) 55–61.
[32] N.A. Rahman, T. Maruyama, H. Matsuyama, Performance of polyethersulfone/tetronic 1307 hollow fiber membrane for drinking water production, J. Appl. Sci. Environ. Sanit. 3 (2008) 1–7.
[33] D.C. Montgomery, J. Wiley, Design and Analysis of Engineering Experiments, in, Wiley, New York, NY, 2001.
[34] M. Zabeti, W.M.A.W. Daud, M.K. Aroua, Optimization of the activity of CaO/Al_2O_3 catalyst for biodiesel production using response surface methodology, Appl. Catal., A 366 (2009) 154–159.
[35] G. Vicente, M. Martinez, J. Aracil, Optimisation of integrated biodiesel production. Part I. A study of the biodiesel purity and yield, Bioresour. Technol. 98 (2007) 1724–1733.
[36] J. Landaburu-Aguirre, E. Pongrácz, P. Perämäki, R.L. Keiski, Micellar-enhanced ultrafiltration for the removal of cadmium and zinc: Use of response surface methodology to improve understanding of process performance and optimisation, J. Hazard. Mater. 180 (2010) 524–534.
[37] R. Gheshlaghi, J. Scharer, M. Moo-Young, P. Douglas, Application of statistical design for the optimization of amino acid separation by reverse-phase HPLC, Anal. Biochem. 383 (2008) 93–102.
[38] J. Sargolzaei, A.H. Moghaddam, J. Shayegan, Statistical assessment of starch removal from starchy wastewater using membrane technology, Korean J. Chem. Eng. 28 (2011) 1–8.
[39] D. Staiger, J.H. Stock, M.W. Watson, The NAIRU, unemployment and monetary policy, J. Econ. Perspect. 11 (1997) 33–49.
[40] S. Mannan, A. Fakhru'l-Razi, M.Z. Alam, Optimization of process parameters for the bioconversion of activated sludge by *Penicillium corylophilum*, using response surface methodology, J. Environ. Sci. 19 (2007) 23–28.
[41] M.S. Hung, J.J. Divoky, A computational study of efficient shortest path algorithms, Comput. Oper. Res. 15 (1988) 567–576.
[42] K. Guerra, J. Pellegrino, J.E. Drewes, Impact of operating conditions on permeate flux and process economics for cross flow ceramic membrane ultrafiltration of surface water, Sep. Purif. Technol. 87 (2012) 47–53.
[43] A. Idris, F. Kormin, M. Noordin, Application of response surface methodology in describing the performance of thin film composite membrane, Sep. Purif. Technol. 49 (2006) 271–280.